

# Unusual Approaches to the Preparation of Heterogeneous Catalysts and Supports Using Water in Subcritical and Supercritical States<sup>1</sup>

A. A. Galkin\*, B. G. Kostyuk\*, N. N. Kuznetsova\*,  
A. O. Turakulova\*, V. V. Lunin\*, and M. Polyakov\*\*

\* Department of Chemistry, Moscow State University, Moscow, 119899 Russia

\*\* Nottingham University, Nottingham, England, United Kingdom

Received August 25, 2000

**Abstract**—The prospective ways of using water in sub- and supercritical states for the preparation of nanocrystal oxide catalysts  $\text{Ce}_{0.5}\text{Zr}_{0.5}\text{O}_2$ ,  $\text{Ce}_{0.1}\text{Y}_x\text{Zr}_{0.9-x}\text{O}_2$ ,  $\text{Zr}_{1-x}\text{Y}_x\text{O}_2$ ,  $\text{Zr}_{1-x}\text{In}_x\text{O}_2$ ,  $\text{La}_2\text{CuO}_4$ , supported catalysts  $\text{Pd/Rh/ZrO}_2$  and  $\text{Pd/Rh/TiO}_2$ , and supports  $\text{CeO}_2$ ,  $\text{ZrO}_2$ ,  $\text{TiO}_2$  are discussed. The proposed technique is characterized by high productivity. It is also ecologically friendly and enables one to obtain multicomponent oxide catalysts with chemical and phase composition and properties that can be changed within large ranges. The physicochemical properties of sub- and supercritical water are discussed. A brief review of the present studies on the use of critical media in various physicochemical processes is given.

In 1822, the French chemist baron Cagniard de Latour discovered the critical point of a substance while performing experiments with different solvents at high temperatures and pressures [1]. The supercritical state of a substance was defined as a state when there is no difference between the liquid and gas phases. After this discovery, the chemistry of supercritical media has been developing rather slowly, and even 70 years later, in 1896, Willard wrote the first detailed review devoted to the properties of a number of substances in a supercritical state [1]. In the 20th century, the trend to enhance the efficiency and ecological safety of various chemical processes stimulated intense studies of the properties of diverse substances under supercritical conditions. Nowadays supercritical liquids are widely used in the processes of extraction and chromatographic separation of chemicals, the production of various materials, and the abatement of toxic liquid wastes [1, 2]. Besides, new possibilities of using supercritical liquids in organic and inorganic syntheses, as well as in homogeneous and heterogeneous catalysis are being developed [3–6]. The characteristics of the critical state (temperature,  $T_{\text{cr}}$ ; pressure,  $P_{\text{cr}}$ ; and density,  $\rho_{\text{cr}}$ ) for most frequently used solvents are given in Table 1 [3, 7]. As can be seen from the table, these characteristics are considerably different: they range from 9°C and 50 atm for ethylene up to 374°C and 220 atm for water.

The permanently growing interest in supercritical liquids arises from their unique physicochemical prop-

erties. Let us trace the changes in the properties of a solvent which take place when approaching the critical point, using water as an example. It should be noted that because of the high values of the critical parameters (see Table 1), water in the critical state is not widely used yet. But, at the same time, it is the cheapest, safest, and most ecologically friendly solvent.

The properties of pure water and water solutions depend strongly on the temperature and pressure. Changes in the thermodynamic properties are reflected in the phase diagrams of water and appropriate multicomponent systems. These changes are associated with changes in the dielectric constant, electric conductivity, ionic strength, and the structure of hydrogen bonds. Finally, changes in the viscosity, density, heat capacity, and diffusion coefficients result in changes of the transport properties of aqueous solutions. It should be noted that all the above-mentioned properties do not alter in a stepwise manner, when approaching the critical point. Even at 300°C and 220 atm, water is similar to acetone, and in the critical state water is a nonpolar solvent that can be mixed with oxygen and hydrocarbons without any limits.

Let us consider the density of water as an example to trace the changes in the properties when approaching the critical state. In the subcritical region, water can exist both in the liquid and gas states, which are separated by a sharp border. At a constant temperature, while changing the pressure, the density of water varies continuously within the intervals of the existence of these two phases. The discontinuity of density is observed only at the gas–liquid interface. In the critical state, this interface disappears, and the density of water

<sup>1</sup> Proceedings of the Seminar in Commemoration of professor Yu.I. Ermakov, Novosibirsk.

is approximately 0.3 g/cm<sup>3</sup> [7]. Water possesses unlimited compressibility near the critical point; that is why even insignificant changes in temperature or pressure in this region allows one to change considerably the density in a wide range. For instance, raising the temperature by 6°C at 220 atm halves the density of water [8]. Other characteristics, such as dielectric constant, ionic strength, viscosity, and heat capacity change in parallel with the changes in density. Therefore, we can operate with the properties of water as a solvent and control the physicochemical processes which take place in water only by changing in a controllable way the water density in sub- and supercritical states.

The ionic strength and the dielectric constant are the most important characteristics for preparing individual and composite oxide catalytic systems in sub- and supercritical water. These properties determine the rates of hydrolysis of inorganic salts in water with further formation of the metal oxides and hydroxides. An increase in the ionic strength of water in the subcritical state, with a simultaneous decrease in its dielectric conductivity, favors the hydrolysis of inorganic compounds [9].

The experiments in sub- and supercritical water are usually performed both in batch reactors and flow-type systems. The batch reactor represents an autoclave fixed inside a powerful heater and equipped with a pressure gauge. Since the discovery of the critical state of substances in the 19th century, the majority of the experiments in sub- and supercritical media have been performed in batch reactors. However, this system is not suitable for the preparation of oxide systems from the corresponding inorganic salts for many reasons. For example, the hydrolysis of acetates leads to the formation of acetic acid. Its partial decomposition is followed by an uncontrollable increase of the pressure in the system. Many multicomponent oxide systems cannot be prepared in batch reactors because of different hydrolysis rates for the metal oxide components composing inorganic salts. Therefore, in this case, gradual autoclave heating results in the separate formation of individual oxides. Besides, the materials prepared in batch systems are usually characterized by a nonuniform particle size distribution.

The main advantage of synthesis in a batch reactor in comparison with flow-type systems is the possibility to control the oxidation states of the elements and to prepare systems with the desirable ratio of phases which contain one element in different oxidation states. For example, copper hydroxycarbonate decomposes into copper(II) oxide (see the diffraction pattern in Fig. 1a):



Oxalic acid under the same conditions decomposes with the formation of carbon monoxide:



The combination of these two reactions in supercritical water ( $T = 385^\circ\text{C}$  and  $P = 350$  atm) allowed us to obtain metallic copper (in the case of an excess of oxalic acid,

**Table 1.** Critical parameters of several solvents [3, 7]

Solvent	$T_{\text{cr}}$ , °C	$P_{\text{cr}}$ , atm	$\rho_{\text{cr}}$ , g/cm <sup>3</sup>
$\text{C}_2\text{H}_4$	9.1	50.41	0.214
Xe	16.5	58.40	1.110
$\text{CO}_2$	30.9	73.75	0.468
$\text{C}_2\text{H}_6$	32.2	48.84	0.203
$\text{N}_2\text{O}$	36.4	72.55	0.452
$\text{NH}_3$	132.3	113.50	0.235
$\text{C}_2\text{H}_5\text{OH}$	240.7	61.37	0.276
$\text{H}_2\text{O}$	373.9	220.60	0.322

Fig. 1d), a mixture of metallic copper and cuprous oxide (at the molar ratio salt : acid = 1 : 2, Fig. 1c), or a mixture of copper(I) and copper(II) oxides (at the molar ratio salt : acid = 3 : 1, Fig. 1b). The content of each phase is determined by the amount of oxalic acid added and, thus, can easily be controlled. Such a technique can be very efficient for the preparation of catalysts and magnetic materials with a specified concentration of paramagnetic centers. However, in any other case of the preparation of oxide systems, it is better to use flow-type reactors. Then, we can obtain nanocrystal materials with a large surface area, which is hard to achieve using conventional methods. Besides, flow type systems exhibit other advantages in comparison with autoclaves: the experimental conditions can easily be controlled and the productivity of the process is rather high.

The group of Professor Arai (Tohoku University, Japan) pioneered the synthesis of nanocrystal metal oxides in sub- and supercritical water. Presently, individual oxides of Ce, Zr, Co, Ni, Fe, Al, and Ti are prepared in this laboratory using a flow-type reactor. Adshiri (a member of Arai's team) synthesized several composite oxides such as  $\text{BaO} \cdot 6\text{Fe}_2\text{O}_3$ ,  $\text{Al}_5(\text{Y} + \text{Tb})_3\text{O}_{12}$ , and  $\text{LiCoO}_2$  in basic media [10]. Recently, the group of Professor Polyakov (Nottingham University, England) prepared a number of composite nanocrystal oxides with the composition  $\text{Ce}_{1-x}\text{Zr}_x\text{O}_2$  in a flow-type reactor in supercritical water without any basic additives [11].

The aim of our work was to develop a technique that allows the preparation of composite oxide nanocrystal catalytic systems using a flow-type reactor and that makes it possible to control the phase composition and physicochemical properties of the catalysts. The activity and selectivity of heterogeneous catalysts are known to be a function of their chemical composition and their micro- and macrostructure. The defectiveness of the crystal and ceramic structure, the surface structure as

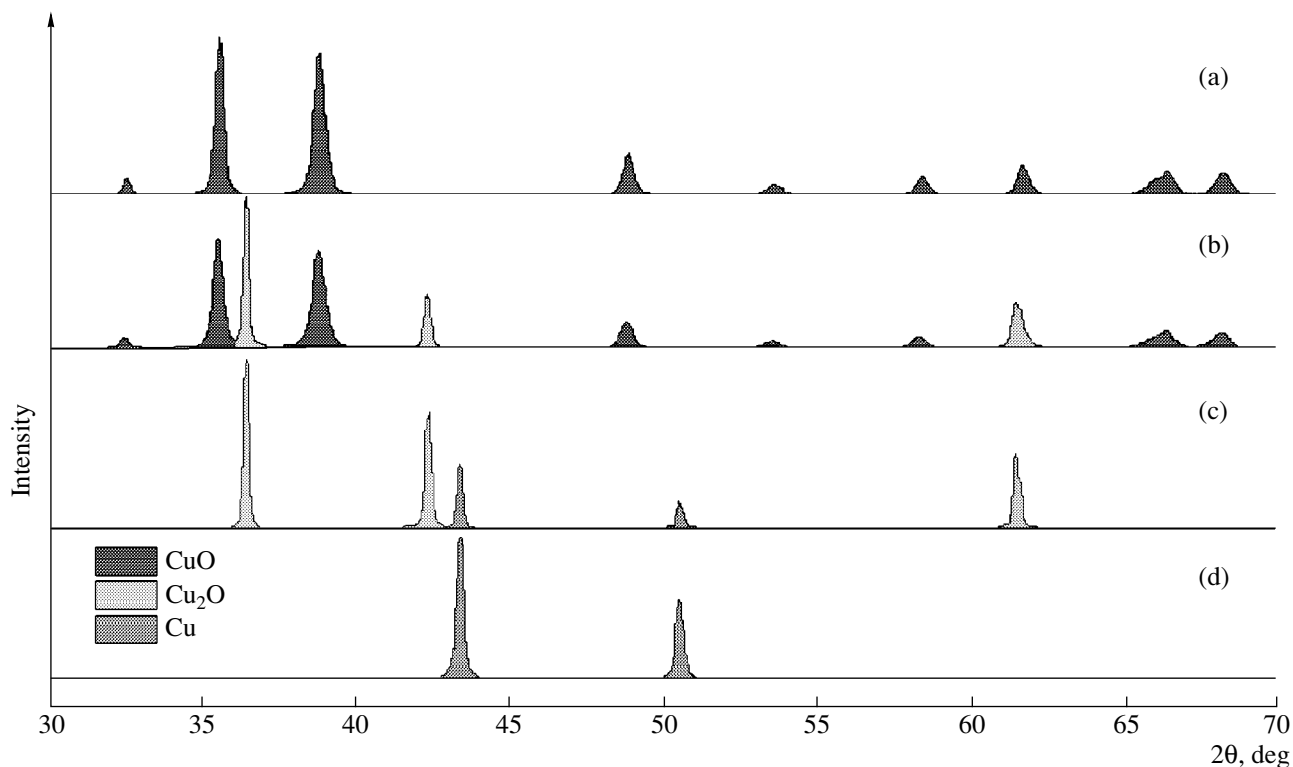
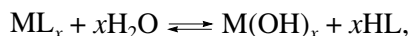


**Fig. 1.** XRD patterns of copper-containing systems obtained in supercritical water in a batch reactor: (a) CuO, (b) CuO + Cu<sub>2</sub>O, (c) Cu<sub>2</sub>O + Cu, and (d) Cu. The experimental conditions are given in the text.

well as the nature of active sites, and the concentration and distribution of admixed phases depend strongly on the synthesis conditions and further thermal treatment of the catalysts. Therefore, we believe that the use of sub- and supercritical water will enable us both to prepare new catalysts and to vary the properties of traditional catalysts and supports.

The scheme of the flow-type system is shown in Fig. 2. The high-pressure pump is used to supply water (10 ml/min) into the system of powerful heaters where it is heated up to a desired temperature (Table 2). The second pump is used to supply an aqueous solution of water salts (feed rate, 5 ml/min; concentration, 0.2 mol/l). Mixing these two flows at the entrance to the reactor results in the rapid hydrolysis of the metal salts with further dehydration of hydroxides according to the following scheme:



where L = NO<sub>3</sub><sup>-</sup>, CH<sub>3</sub>COO<sup>-</sup>, M = Ce, Zr, Ti, Cu, Y, In, Pd, and Rh.

After that the colloid solution of metal oxides is cooled to room temperature, separated, and evaporated on the rotor. A constant pressure in the system is kept using a back-pressure valve.

The conditions of all experiments are summarized in Table 2. Zirconium oxide and composite materials based on zirconium oxide were prepared in supercritical water at 380°C and 250 atm. The residence time was 4.5 s. Cerium and titanium oxides as well as Pd–Rh catalysts supported on titanium oxide were prepared in subcritical water. In this case, the residence time was 1.5–2 times higher. The salt concentration 0.2 mol/l was shown to be the optimal for the reaction mixture. The feed rates were 10 and 5 ml/min for water and a solution of metal salts, respectively.

It was mentioned previously that the hydrolysis of a metal salt in sub- and supercritical water is followed by the formation of a colloid solution of corresponding oxides. The microphotograph of zirconium oxide prepared by the evaporation of such a colloid solution is presented in Fig. 3. The size of zirconium oxide particles is as low as 3–5 nm. All the prepared samples show a nanocrystal structure with a narrow particle size distribution. The maximum size of the particles is 7–9 nm in the case of titanium oxide systems.

By varying the experimental conditions, we can change the particle size of the synthesized materials. For example, a temperature rise from 230 to 380°C during the synthesis of TiO<sub>2</sub> leads to a simultaneous increase in the size of oxide particles from 7–9 to 16–18 nm. The specific surface area, at the same time, decreases from 200 to 50 m<sup>2</sup>/g. The processes of titanium oxide recrys-

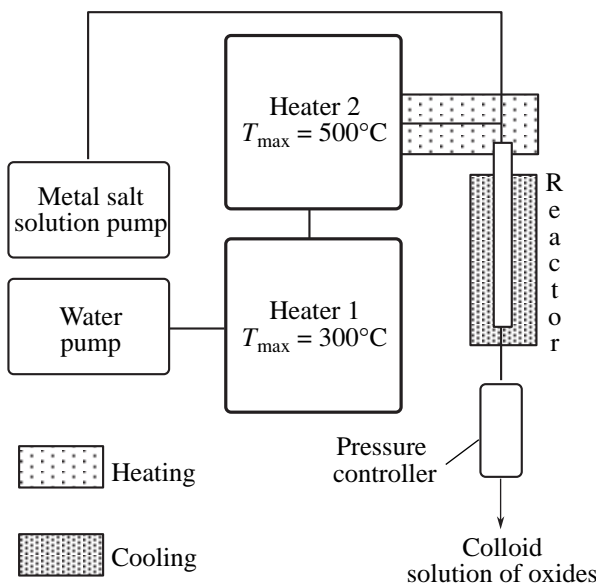


**Fig. 2.** The scheme of the flow-type reaction system operating in sub- and supercritical conditions.

tallization most probably occur at elevated temperatures, thus resulting in the growth of the particles. The same phenomena are observed when the salt concentration increases.

Let us analyze the phase composition of oxides prepared in sub- and supercritical water. The XRD patterns of Ce, Ti, and Zr oxides are shown in Fig. 4. Zirconyl nitrate, cerium ammonium nitrate, and titanium isopropoxyacetate were used as precursors. According to the XRD analysis, the crystallization of titanium oxide in subcritical water occurs with the formation of the tetragonal modification, the lattice of  $\text{CO}_2$  has cubic symmetry, and zirconium oxide forms a mixture of the tetragonal and monoclinic modifications with the ratio approximately 1 : 1.

The tetragonal and cubic modifications of  $\text{ZrO}_2$  are known to be metastable at normal conditions [12]. At the same time, the problem of the stabilization of such structures at low temperatures is of a great importance, especially in the case of oxidation catalysts, because the higher symmetry of the crystal lattice of an oxide favors the mobility of oxygen in the volume of the catalyst. A number of transition and alkali-earth metals are used for the stabilization of the tetragonal and cubic  $\text{ZrO}_2$  modifications. Several experiments on the preparation of binary oxide systems, containing indium, yttrium, and cerium in addition to zirconium were performed in supercritical water with the purpose of revealing the possibility of such stabilization.

An increase in the indium content in the case of the Zr-In systems results in the growth of the ratio between the tetragonal and monoclinic modifications of  $\text{ZrO}_2$ . Nevertheless, the complete stabilization of the tetragonal structure is not achieved even at indium concentra-

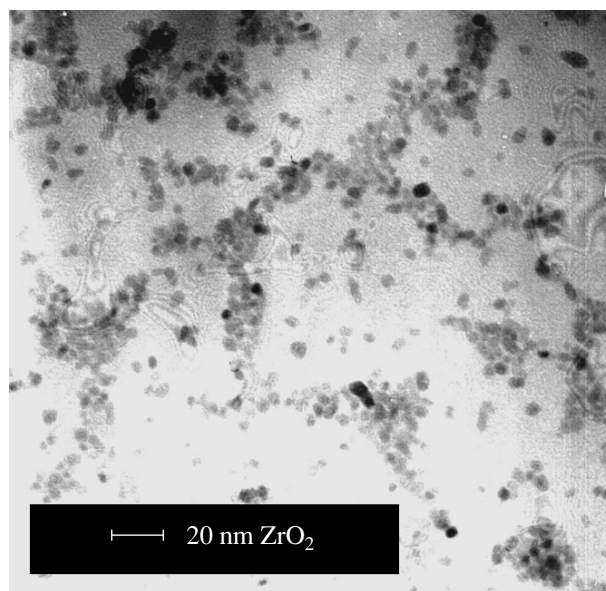


**Fig. 3.** Electronic micrographs of  $\text{ZrO}_2$  prepared in supercritical water.

tions up to 10%. The synthesis in supercritical conditions is likely followed by the incorporation of only a part of indium atoms into the lattice of zirconium oxide, and individual indium oxide is formed in parallel with the formation of the binary system  $\text{Zr}_{1-x}\text{In}_x\text{O}_2$ .

The situation is much better in the case of the Zr-Y system (Fig. 5). An yttrium concentration of 10% is sufficient for the predominant formation of the tetragonal modification of  $\text{ZrO}_2$ . The content of the mono-

**Table 2.** Experimental conditions for the preparation of oxide-type catalysts in sub- and supercritical water

Sample	$T, ^\circ\text{C}$	$P, \text{atm}$	$\rho, \text{g/cm}^3$	Reaction time, s
$\text{ZrO}_2$	380	250	0.446	4.5
$\text{Zr}_{1-x}\text{In}_x\text{O}_2$	380	250	0.446	4.5
$\text{Zr}_{1-x}\text{Y}_x\text{O}_2$	380	250	0.446	4.5
$\text{Ce}_{0.5}\text{Zr}_{0.5}\text{O}_2$	380	250	0.446	4.5
$\text{Ce}_{0.1}\text{Y}_x\text{Zr}_{0.9-x}\text{O}_2$	380	250	0.446	4.5
1% Rh-Pd/ $\text{ZrO}_2$	380	250	0.446	4.5
10% Rh-Pd/ $\text{ZrO}_2$	380	250	0.446	4.5
$\text{CeO}_2$	330	250	0.681	6.8
$\text{TiO}_2$	230	250	0.847	8.5
1% Rh-Pd/ $\text{TiO}_2$	230	250	0.847	8.5

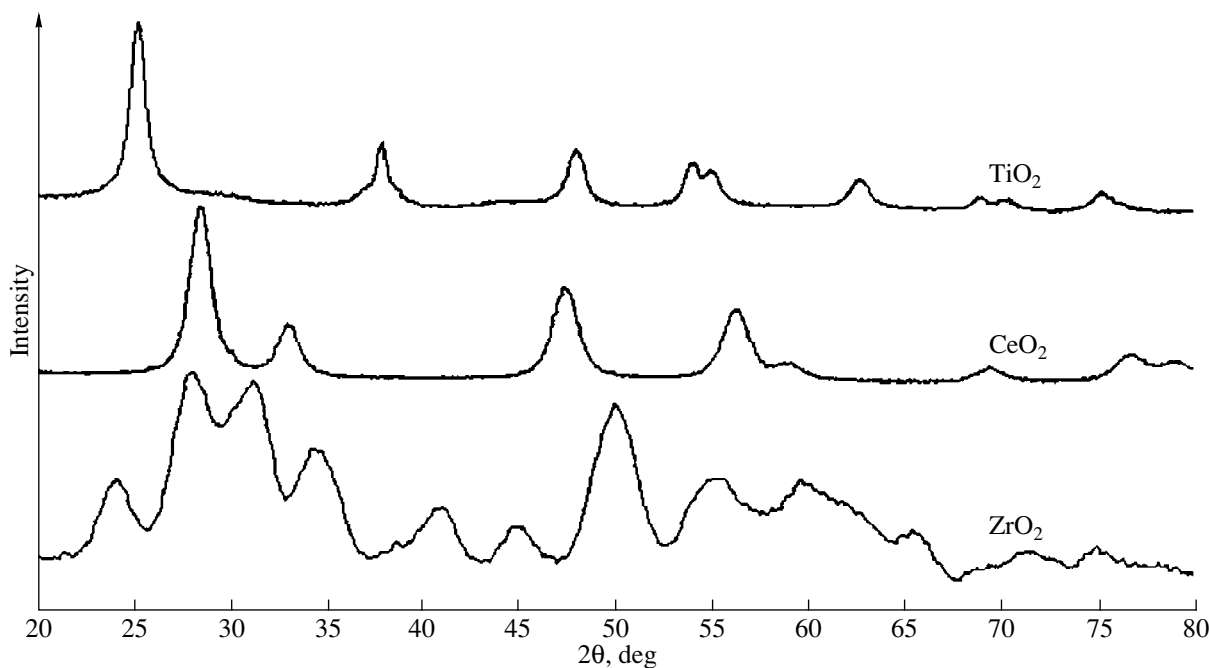


**Fig. 4.** XRD patterns of Ce, Ti, and Zr oxides obtained in supercritical water.

clinic phase is rather low and we hope that further optimization of experimental conditions will enable us to exclude the formation of the monoclinic modification.

It is quite possible that the formation of the cubic  $ZrO_2$  phase instead of the tetragonal modification explains the shape of the XRD patterns presented in Fig. 5. Such significant line broadening makes difficult the unequivocal identification of the XRD patterns. Additional information can be obtained by Raman spectroscopy. Using this technique, we demonstrated the principal possibility of the stabilization of the cubic phase in supercritical water for a number of multicomponent oxide catalysts based on  $ZrO_2$ . Cubic symmetry is typical for Ce-Zr solid solutions with a metal ratio of 1 : 1, Zr-Rh systems containing 10% Rh, and ternary Ce-Zr-Y systems containing 10% Ce and 10% Y. All these composite oxides are single-phase nanocrystal systems with a developed specific surface area.

The specific surface areas of all prepared oxide catalysts are given in Table 3. Titanium oxide and Rh-Pd catalysts supported on titanium oxide have the maximum surface area (approximately  $200 \text{ m}^2/\text{g}$ ). The specific surface area of the systems based on zirconia is varied in the range  $140$ – $170 \text{ m}^2/\text{g}$ . For  $CeO_2$ , the surface area does not exceed  $110 \text{ m}^2/\text{g}$ . It should be emphasized that all the samples under discussion are crystalline systems, and it is almost impossible to obtain catalysts with such a high surface area by using traditional techniques such as coprecipitation, impregnation, sol-gel synthesis, etc.

It is important that oxides prepared in supercritical water display high thermal stability and have almost no

tendency to sintering. The XRD patterns of three  $ZrO_2$  samples prepared in (a) supercritical water and after thermal treatment at (b)  $600$  and (c)  $900^\circ\text{C}$  for 1 h are presented in Fig. 6. It can be seen that the calcination of the sample at  $600^\circ\text{C}$  does not change the phase composition and surface area. Even after thermal treatment at  $900^\circ\text{C}$ , the XRD lines are rather wide, which is typical for small oxide particles. The specific surface area diminishes two times and is only  $90 \text{ m}^2/\text{g}$ . Even such a low value of the surface area is considerably higher than the specific surface area of the zirconium oxide systems prepared by precipitation with ammonia from zirconium-containing solutions. The content of the tetragonal modification of  $ZrO_2$  significantly increases after calcination at  $900^\circ\text{C}$ . Therefore, the stabilization of the metastable tetragonal modification is observed at much lower temperatures in the case of the samples prepared in supercritical conditions.

Thus, the preparation of oxide catalysts in sub- and supercritical water enables one to obtain nanocrystal homogeneous materials with a high surface area. However, this technique has also one significant disadvantage. The elemental analysis of all prepared samples is shown in Table 3. As can be seen from Table 3, the content of carbon and nitrogen in the samples is much higher than expected. It can be caused by either the presence of unreacted starting materials in prepared oxides or the adsorption of nitric or acetic acids formed during the hydrolysis of metal salts.

To clarify the origin of this phenomenon, we performed a number of thermal gravimetric analyses for several samples. The results are presented in Fig. 7. The

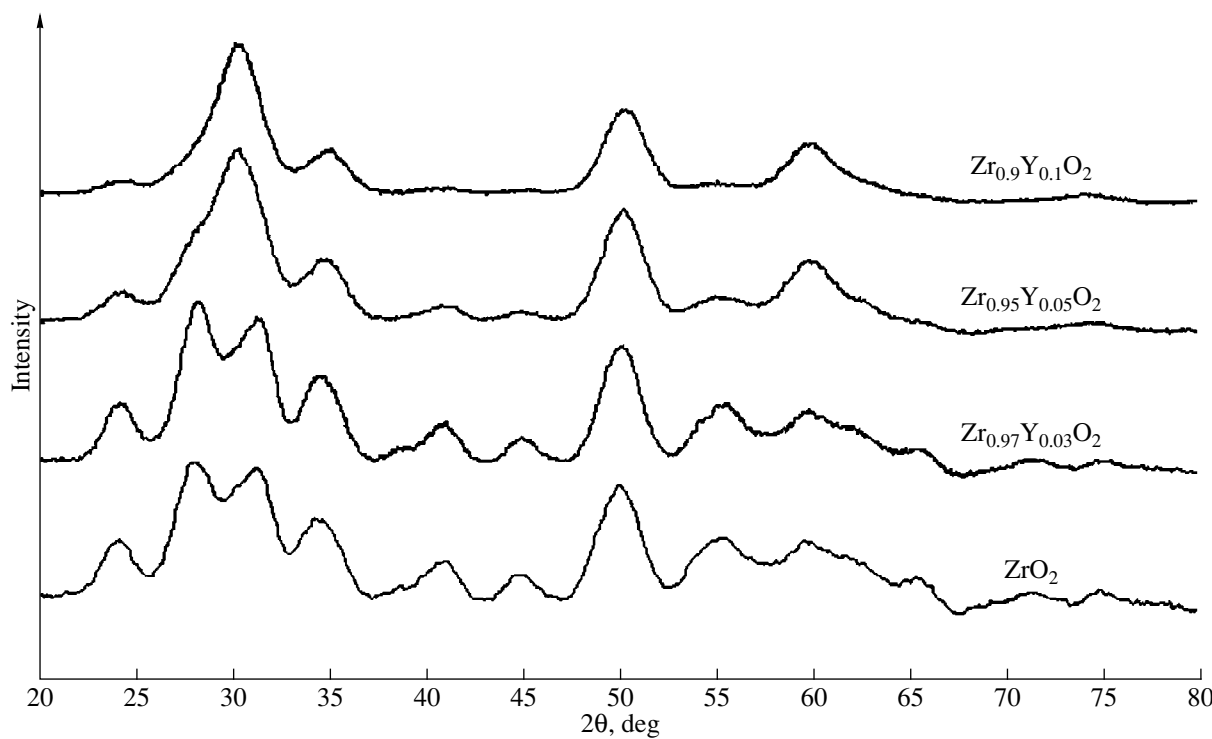


Fig. 5. Dependence of the phase composition of  $\text{ZrO}_2$  samples prepared in supercritical water on the yttrium content.

DTG curve of zirconium oxide (upper curve) exhibits two peaks in the temperature range up to 600°C corresponding to weight loss at 140 and 420°C. The first peak is likely the result of water elimination. The second weight loss can be explained by either the decomposition of unreacted zirconium nitrate or the desorp-

tion of nitric acid. The lower curve in Fig. 7 corresponds to the decomposition of zirconyl nitrate, which was used as a precursor. The maximum rate of its decomposition is observed at 225°C. The absence of this maximum in the DTG curve of  $\text{ZrO}_2$  indicates that the increased nitrogen content can be accounted for by

Table 3. Specific surface areas and the content of carbon, hydrogen, and nitrogen in the catalysts prepared in sub- and supercritical conditions

Sample	$S, \text{m}^2/\text{g}$	Element content, %		
		C	H	N
$\text{ZrO}_2$	163–172	Not found	0.09–0.89	0.85–1.67
$\text{Zr}_{1-x}\text{In}_x\text{O}_2$	135–154	0.22–0.32	0.37–0.55	1.45–1.84
$\text{Zr}_{1-x}\text{Y}_x\text{O}_2$	147–161	0.14–0.44	0.73–0.84	1.54–2.09
$\text{Ce}_{0.5}\text{Zr}_{0.5}\text{O}_2$	153	Not found	0–0.14	1.06–1.13
$\text{Ce}_{0.1}\text{Y}_x\text{Zr}_{0.9-x}\text{O}_2$	115–164	0.25–0.44	0.31–0.61	1.49–1.51
1% Rh–Pd/ $\text{ZrO}_2$	158	0.12	0.24	0.98
10% Rh–Pd/ $\text{ZrO}_2$	141–159	0.16–0.30	0.63–0.80	0.97–1.11
$\text{CeO}_2$	110	Not found	Not found	1.78–1.82
$\text{TiO}_2$	189–201	0.41–3.64	0–0.65	Not found
1% Rh–Pd/ $\text{TiO}_2$	195–213	2.52–4.27	0.32–0.64	0–1.20

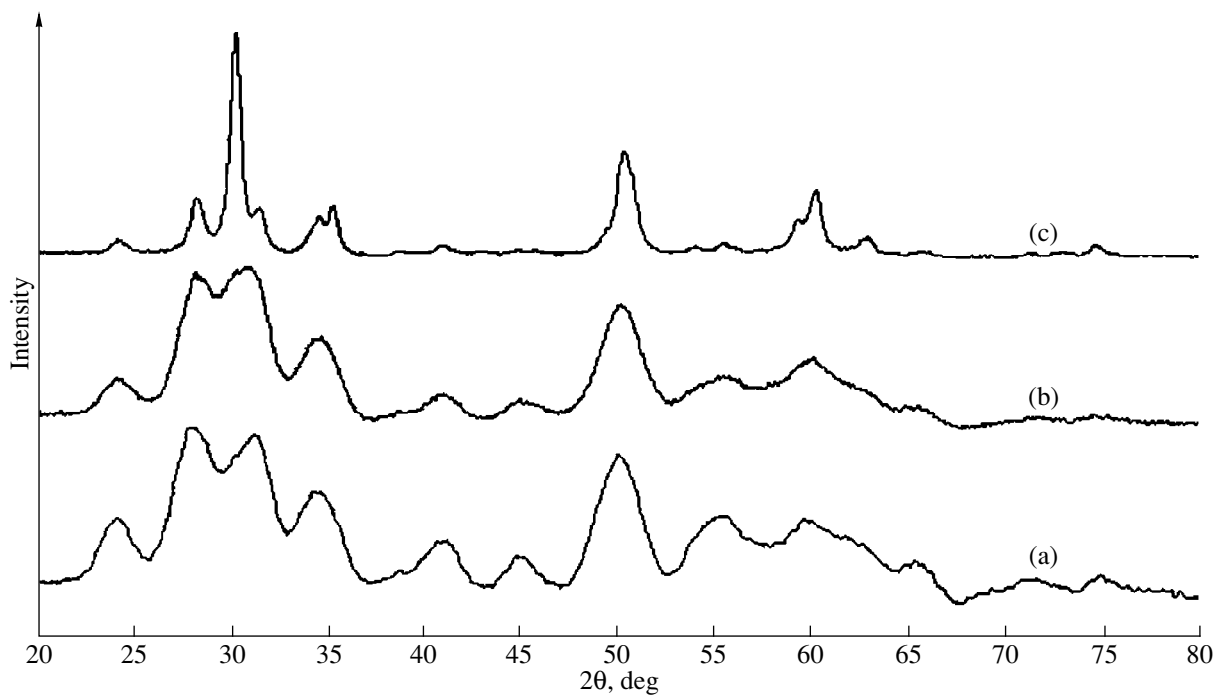


**Fig. 6.** XRD patterns of  $\text{ZrO}_2$  samples: (a) fresh sample prepared in supercritical water, (b) after thermal treatment at 600 and (c) 900°C.

the adsorption of nitric acid rather than by the presence of unreacted zirconyl nitrate. Thermal treatment of all the obtained oxide samples at 600°C results in the complete elimination of all carbon and nitrogen species from the surface according to the data of elemental analysis.

Presently we are studying the catalytic and physicochemical properties of oxide systems prepared in sub- and supercritical water. The preliminary data testify that such a method of catalyst preparation allows one to vary the properties of the catalysts in a wide range. The

temperature-programmed reduction (TPR) curves of three samples of zirconium oxide and rhodium and palladium zirconia-based systems containing 10% of each metal are shown in Fig. 8. It is known from the literature [13] that  $\text{ZrO}_2$  cannot be reduced at temperatures below 1000°C, but in our case, three steps of reduction are observed in this region, and the first reduction peak is observed at 232°C. After introducing rhodium in the catalyst, the consumption of hydrogen increases considerably, and this fact is in agreement with the literature data [14]. The most interesting results are found in the case of palladium-containing samples, where a sufficient hydrogen uptake begins at room temperature, and at 70°C, when the desorption of hydrogen begins.

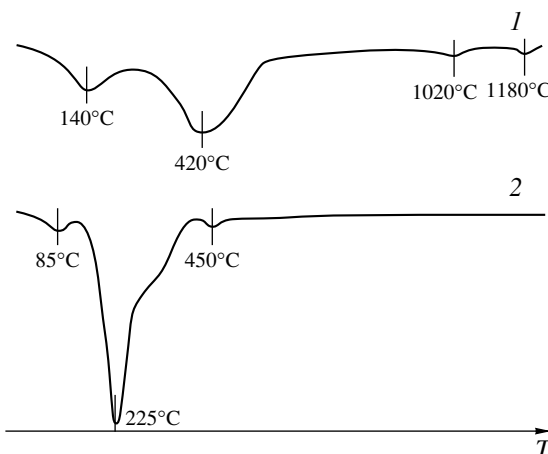


**Fig. 7.** DTG curves of (1)  $\text{ZrO}_2$  sample prepared in supercritical water and (2) zirconyl nitrate.

The contents of  $\text{Zr}^{3+}$  ions in the samples prepared either by using supercritical water or by the traditional coprecipitation technique are given in Table 4. The  $\text{Zr}^{3+}$  cations are considered to be the active sites in the Fischer-Tropsch process [15]. It is well known that the content of  $\text{Zr}^{3+}$  cations in zirconium oxide prepared by traditional techniques is very low even after thermal vacuum treatment and increases only after the introduction of modifying additives [16]. However, in the case of the supercritical samples, the concentration of  $\text{Zr}^{3+}$  cations is rather high even in nonactivated samples, and it is ten times higher than that in the Ce-Zr-Y systems prepared by coprecipitation. The content of  $\text{Zr}^{3+}$  ions in the supercritical samples increases considerably after the introduction of the modifying additives. The concentration of paramagnetic sites in the Ce-Zr system is

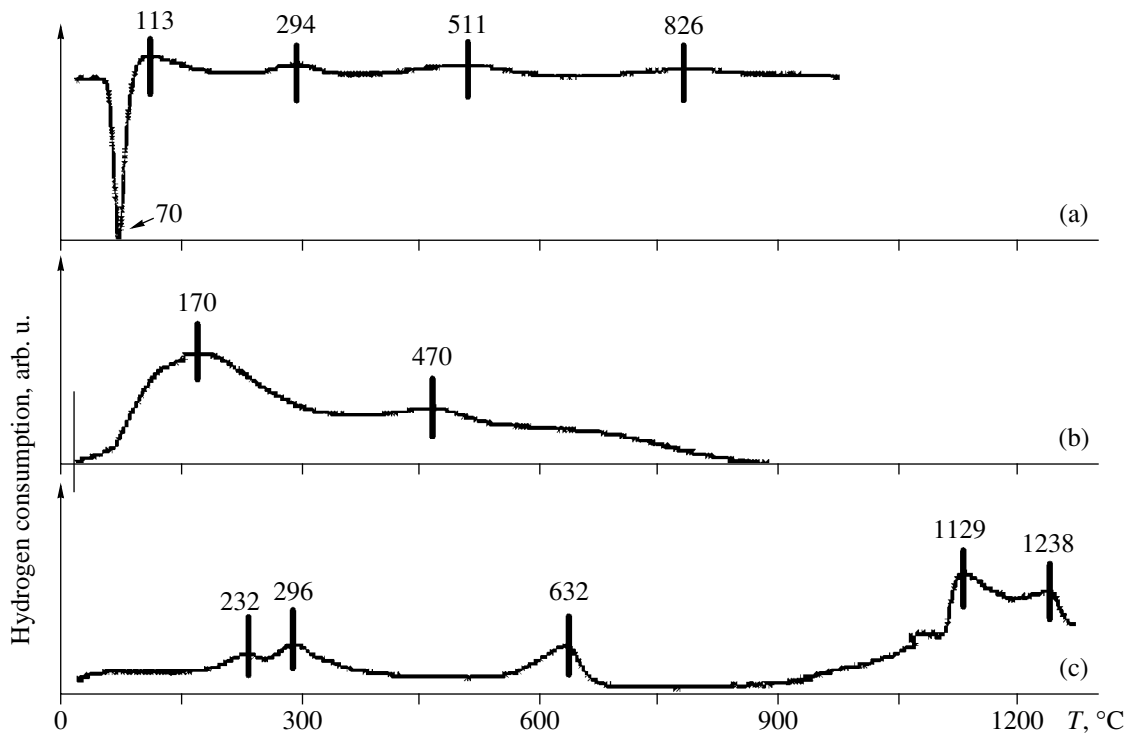


**Fig. 8.** TPR curves for zirconium-based samples prepared in supercritical water: (a) 10% Pd/ZrO<sub>2</sub>, (b) 10% Rh/ZrO<sub>2</sub>, and (c) ZrO<sub>2</sub>. Temperatures (°C) of maximum hydrogen consumption (desorption) are shown above the curves.

two orders higher than in the Ce–Zr–Y samples prepared by conventional methods.

The use of supercritical water is especially effective for the preparation of perovskite-type catalysts. Perovskites are usually prepared by calcination at 1000–1100°C [17]. The specific surface area of such catalysts is usually rather low, and thus they cannot be effectively used in real catalytic processes. Several other techniques such as sol–gel synthesis, coprecipitation, spray drying, and cryochemical techniques, which allow one to diminish the temperatures characteristic for precursor decomposition, are labor-consuming and unprofitable on an industrial scale.

Using lanthanum cuprate as an example, we had shown that the preparation of perovskite-type oxides in supercritical water made it possible to increase the surface area 50 times, as well as to optimize oxygen transfer processes in the volume of the catalyst and to improve its catalytic properties in the oxidation reactions [17].

In the case of lanthanum cuprate, the phase of the perovskite type is not formed directly in supercritical conditions. The hydrolysis of a stoichiometric solution of copper and lanthanum acetates yields a highly dispersed precursor, which contains copper oxide and lanthanum hydroxide. The calcination of this precursor at as low a temperature as 600°C results in the formation of homogeneous lanthanum cuprate.

TPR curves of two La<sub>2</sub>CuO<sub>4</sub> samples, which were prepared either by (a) a ceramic technique or (b) by using supercritical water are presented in Fig. 9. In both cases, the first peak of hydrogen consumption is connected with the elimination of weakly bonded oxygen from the volume of the catalyst, and the second one corresponds to the phase decomposition of the sample followed by the formation of copper and lanthanum oxides. The total hydrogen uptake is the same for both catalysts, but in the case of the supercritical sample, the elimination of weakly bonded oxygen is observed at a temperature 100°C lower and the process occurs faster than in the case of ceramic lanthanum cuprate. This opens up new possibilities for the preparation of effective catalysts in supercritical water, which can be used as the sources of active oxygen.

The increase of oxygen mobility in the supercritical sample of La<sub>2</sub>CuO<sub>4</sub> is explained by the smaller particle size in the catalyst due to the use of a more homogeneous precursor obtained in supercritical water and lower calcination temperatures.

It was shown that the La<sub>2</sub>CuO<sub>4</sub> sample prepared in supercritical water reveals unusual catalytic properties in the reaction of CO oxidation in a pulse microcatalytic system. In the case of the stoichiometric CO and oxygen mixture, the activity of the supercritical sample increases ~2.5 times in comparison with ceramic lanthanum cuprate due to its considerably larger surface area. If the pulses of the reagents are separated in time, the rate of CO oxidation on the supercritical sample

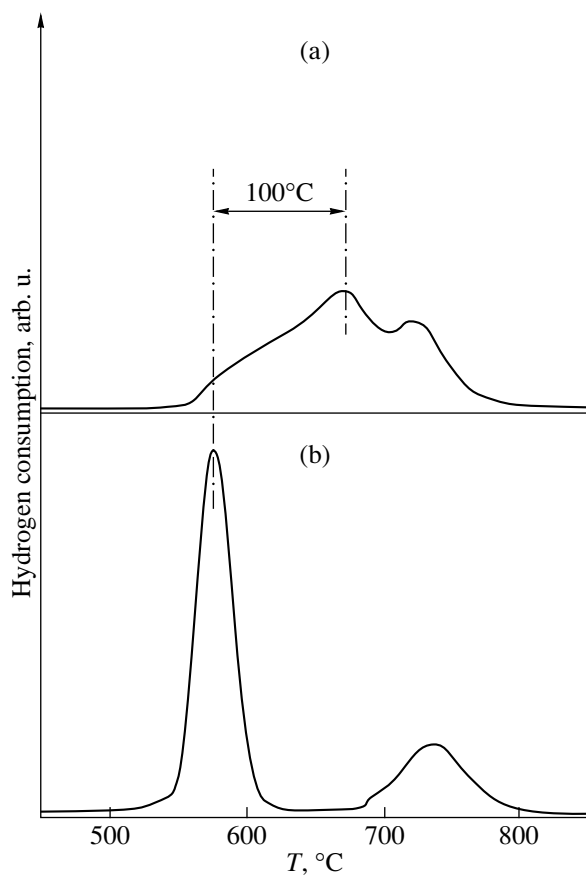


**Fig. 9.** TPR curves of the  $\text{La}_2\text{CuO}_4$  sample prepared by (a) ceramic technique and (b) using supercritical water.

increases  $\sim 8$  times because of the higher oxygen mobility [17].

Therefore, the use of supercritical water creates prospective ways for the preparation of a variety of new catalysts and supports. Note that water in the supercrit-

**Table 4.** The results of the investigation of Zr-containing samples by ESR spectroscopy

$[\text{Zr}^{3+}] \times 10^{17}$ , spin/g		
I. Oxides obtained in supercritical water		
	nonactivated	activated*
$\text{ZrO}_2$	2.5	3.6
$\text{Ce}_{0.1}\text{Y}_{0.06}\text{Zr}_{0.84}\text{O}_2$	1.1	2.0
$\text{Ce}_{0.1}\text{Y}_{0.1}\text{Zr}_{0.8}\text{O}_2$	2.6	2.9
$\text{Ce}_{0.5}\text{Zr}_{0.5}\text{O}_2$	3.8	11.0
II. Oxides prepared by coprecipitation [16]		
$\text{ZrO}_2$	Not found	Not found
$\text{Ce}_{0.1}\text{Y}_{0.06}\text{Zr}_{0.84}\text{O}_2$	Not found	0.1

\* Standard thermal vacuum treatment: first stage,  $T = 550^\circ\text{C}$ , air, 2 h; second stage,  $T = 550^\circ\text{C}$ ,  $P = 10^{-5}$  torr, 2 h.

ical state mixes with oxygen and hydrocarbons without any restrictions, therefore, homogeneous and heterogeneous catalytic reactions in sub- and supercritical water could be of great interest. Moreover, catalysts prepared in nonequilibrium sub- and supercritical conditions would reveal proper stability in supercritical conditions.

## ACKNOWLEDGMENTS

We would like to thank L.N. Ikryannikova and G.L. Markaryan for their assistance in the investigation of the samples by ESR spectroscopy. This work was supported by Russian Foundation for Basic Research and INTAS, joint project no. IR-97-0402.

## REFERENCES

1. McHugh, M.A. and Krukonis, V.J., *Supercritical Fluid Extraction: Principles and Practice*, Boston: Butterworth-Heinemann, 1994.
2. Pisharody, S.A., Fisher, J.W., and Abraham, M.A., *Ind. Eng. Chem. Res.*, 1996, vol. 35, no. 12, p. 4471.
3. Baiker, A., *Chem. Rev.*, 1999, vol. 99, p. 453.
4. Savage, P.E., *Chem. Rev.*, 1999, vol. 99, p. 603.
5. Jessop, P.G., Ikariya, T., and Noyori, R., *Chem. Rev.*, 1999, vol. 99, p. 475.
6. Adschari, T., Kanazawa, K., and Arai, K., *J. Am. Ceram. Soc.*, 1992, vol. 75, no. 4, p. 1019.
7. Van Eldik, R. and Hubbard, C.D., *Chemistry under Extreme or Non-Classical Conditions*, New York: Wiley-Spectrum, 1997.
8. Schmidt, E., *Properties of Water and Steam in SI-Units*, Berlin: Springer, 1969.
9. Kritzer, P., Boukis, N., and Dinjus, E., *J. Supercrit. Fluids*, 1999, vol. 15, p. 205.
10. Adschari, T., *Proc. 5th Int. Symp. on Supercritical Fluids*, Atlanta, 2000.
11. Cabanas, A., Darr, J.A., Lester, E., and Piliakoff, M., *Chem. Commun.*, 2000, no. 7, p. 901.
12. Murav'eva, G.P., Fionov, A.V., Lunina, E.V., *et al.*, *Dokl. Akad. Nauk*, 2000, vol. 371, no. 1, p. 52.
13. Hoang, D.L., Berndt, H., and Lieske, H., *Catal. Lett.*, 1995, vol. 31, nos. 2-3, p. 165.
14. Guglielminotti, E., Giannello, E., Pinna, F., *et al.*, *J. Catal.*, 1994, vol. 146, no. 2, p. 422.
15. Wen, L., Yuanqi, Y., Liangbo, F., and Peiju, Z., *Chin. Chem. Lett.*, 1996, vol. 7, no. 3, p. 269.
16. Markaryan, G.L., Ikryannikova, L.N., Muravieva, G.P., *et al.*, *Colloids Surf. A*, 1999, vol. 151, p. 435.
17. Galkin, A.A., Kostyuk, B.G., Lunin, V.V., and Poliakoff, M., *Angew. Chem. Int. Ed. Engl.*, 2000, vol. 39, no. 15, p. 2738.